

NANO EXPRESS

Open Access



Hydrogen Peroxide Sensing Based on Inner Surfaces Modification of Solid-State Nanopore

Libo Zhu, Dejian Gu and Quanjun Liu*

Abstract

There are many techniques for the detection of molecules. But detection of molecules through solid-state nanopore in a solution is one of the promising, high-throughput, and low-cost technology used these days. In the present investigation, a solid-state nanopore platform was fabricated for the detection of hydrogen peroxide (H_2O_2), which is not only a label free product but also a significant participant in the redox reaction. We have successfully fabricated silicon nitride (Si_3N_4) nanopores with diameters of ~ 50 nm by using a focused Ga ion beam, the inner surface of the nanopore has been modified with horseradish peroxidase (HRP) by employing carbodiimide coupling chemistry. The immobilized HRP enzymes have ability to induce redox reactions in a single nanopore channel. Moreover, a real-time single aggregated $ABTS^{++}$ molecular translocation events were monitored and investigated. The designed solid-state nanopore biosensor is reversible and can be applied to detect H_2O_2 multiple times.

Keywords: Sensor, Nanopore, Hydrogen Peroxide, Horseradish Peroxidase (HRP)

Background

Nanopore detection technology originates from Coulter counter [1] and cell ion channel [2]. Nanopore detects charged molecules present in a solution passing through it. The appearance of the molecules in nanopore can change the conductance of the pore apparently, consequently a change in the current signal. The change in the current provides the information about the sizes and concentration of the molecules inside the pore, to reveal the dynamics process of the molecules translocation behaviours [3]. Some nanoscale objects can be detected using a nanopore, such as nanoparticles [4–6], viruses [7–9], protein molecules [10–13] and DNA sequences [14–17]. Nanopores are of two types. Biology nanopore and the solid-state nanopore. The biology nanopore has lower signal to noise ratio (SNR), and higher resolution. Small and unfolded proteins can be detected by using biology nanopores [18–23]. Solid-state nanopore is size adjustable and has higher stability. The solid-state nanopore is normally drilled on a film, this film divides the

fluidic cell into two parts [24]. A biased voltage is applied across a thin membrane containing a nanopore, resulting in an ionic current from one cell to another [25]. Protein molecules including folded and unfolded structures are detected and analyzed by solid-state nanopore [26–29]. The interaction of proteins can also be detected using solid-state nanopore [30, 31]. Moreover, it has ability to detect protein kinetics [32, 33]. In order to solve the limits on the detection range, chemically modified solid-state nanopores have been applied extensively [34–39], chemically modified solid-state nanopores have been applied to detect single-stranded DNA [40] and proteins [41].

A lot of quantitative methods have already been applied for the detection of H_2O_2 , most of them are based on spectrometry [42–45], chemoluminescence [46–49], amperometry [50–53] and electrochemistry [54–57]. The conventional spectrometric and chemoluminescence methods are commonly time-consuming and costly. The solid-state nanopore sensor has low consumption and simple structure, and can be used to detect small molecules.

Here, we present a type solid-state nanopore that was modified with horseradish peroxidase (HRP). The HRPs

* Correspondence: lqj@seu.edu.cn

State Key Laboratory of Bioelectronics, School of Biological Science and Medical Engineering, Southeast University, No. 2, Sipailou, Nanjing 210096, People's Republic of China

were immobilized on the inner surface of solid-state nanopore, the immobilized HRP remained active in redox reaction that occurred inside a single nanopore channel in the presence of H_2O_2 [58]. The $ABTS^{•+}$ produced in redox reaction would aggregate, then the aggregated $ABTS^{•+}$ passed through nanopore. The translocation events can be detected. For the hydrogen peroxide detection, the structure of solid-state is simple, and it can detect the aggregated $ABTS^{•+}$ by using low reagent consumption. This horseradish peroxidase (HRP) enzymes modification solid-state nanopore can accomplish the hydrogen peroxide (H_2O_2) sensing indirectly, through the aggregated $ABTS^{•+}$ detection. It has instructive significance for single molecule detection and molecules assembly inner solid-state nanopore.

Methods

Chemicals and Materials

The Horseradish Peroxidase (HRP) molecule (1mg mL^{-1} , Enzyme Commission No.1.11.1.7, 44 kDa) was purchased from Xiya Reagent (Chengdu, China). The sample (HRP) was dissolved in $0.02\ \mu\text{m}$ filtered $0.1\ \text{M}$ PBS, stored at $4\ ^\circ\text{C}$, and employed within two days of preparation. Potassium chloride (KCl), N-(3-dimethylaminopropyl)-N'-ethylcarbodiimide (EDC), N-hydroxysuccinimide (NHS) and 2,2'-Azino-bis (3-ethylbenzothiazoline-6-sulfonic acid) ((ABTS), 98%) were purchased from DiBo chemical technology co., LTD (Shanghai, China). Hydrogen peroxide (H_2O_2 , 30%) was bought from Sinopharm Chemical Reagent Co., Ltd. (3-Aminopropyl)triethoxysilane (3-APTES) was purchased from Sigma-Aldrich (St. Louis, MO, USA). Experiments were conducted using ultrapure water from a Milli-Q water purification system (resistivity of $18.2\ \text{M}\Omega/\text{cm}$, $25\ ^\circ\text{C}$, Millipore Corporation, Billerica, MA, USA) and was filtered through $0.02\ \mu\text{m}$ in a FEI Strata 201 FIB system (FEI Co., Hillsboro, OR, USA), a Zetasizer (Malvern Zetasizer Nano ZS), and an Axopatch 700B (Molecular Devices, Inc., Sunnyvale, CA, USA). The pictures of our used instruments were added to the supplementary material (see Additional file 1: Figure S1).

Solid-State Nanopore Fabrication and Electrical Measurements

First, a thin membrane of Si_3N_4 (100 nm thickness) was deposited on a Si substrate having $300\ \mu\text{m}$ thickness. Followed by photolithography (the open window size is $500 \times 500\ \mu\text{m}^2$). Then, the surface of the membrane was bombarded with Ga⁺ ions using a FEI Strata 201 FIB system (FEI Co., Hillsboro, OR, USA) at an acceleration potential of 30 kV, while the current was measured as 1 pA. The milling time was 1.5 s under a spot mode. Finally, the solid-state nanopore chips were obtained and cleaned in fresh prepared piranha solution at $80\ ^\circ\text{C}$ for

30 min, followed by rinsing with ultrapure water. After cleaning, the chip was assembled in a custom-built Teflon cell with two Viton o-rings to separate the two sides of chip, and forming two reservoirs to ensure the only path for ionic current through the nanopore. The pictures of our used apparatus were added to the supplementary material (see Additional file 1: Figure S2). Electrodes (Ag/AgCl) were connected to the fluidic cell and a patch clamp amplifier (Axopatch 700B, Molecular Devices, Inc., Sunnyvale, CA, USA) that made the ionic current measurable under constant voltages, with 100 kHz sampling rate for signals. The amplifier internal low-pass eight-pole Bessel filter was set at 10 kHz [3]. The whole instrument was placed in a double Faraday cage enclosure.

Results and Discussion

Immobilization of Nanopore with HRP

The selected nanopore with a diameter of $\sim 50\text{nm}$ was immersed in piranha solution at $80\ ^\circ\text{C}$ for 30 min. After treating with piranha solution, the inner surface of nanopore was able to take silicon hydroxyl groups. Subsequently, the entire thin film was activated with (3-Aminopropyl)triethoxysilane (3-APTES). As a result of treating with 3-APTES, the amino ($-NH_2$) groups were generated on the surface of film.

After activation with (3-Aminopropyl)triethoxysilane (3-APTES), the nanopore chip was brought into $0.1\ \text{M}$ PBS solution of N-(3-dimethylaminopropyl)-N'-ethylcarbodiimide (EDC) ($10\ \text{mM}$) and N-hydroxysuccinimide (NHS) ($20\ \text{mM}$). Thereafter, the nanopore chip was introduced to horseradish peroxidase (HRP) ($10\ \text{ng/ml}$). According to previous research results of our group [3], with different salt concentration from 0.1 to $2\ \text{M}$ KCl, pH 7.0, HRP did not aggregate. On account of the pI value of horseradish peroxidase being 4.3 ± 0.2 , we also proved that the HRP did not aggregate in $0.1\ \text{M}$ KCl pH 6.0 and pH 7.0. The EDC reagent activated the carboxyl ($-COOH$) groups of HRP into a highly reactive *o*-acylisourea intermediate. Furthermore, the intermediate was further converted into a more stable succinimidyl amine-reactive ester in the presence of NHS [58]. Resulting, in covalent coupling of the intermediate with the ($-NH_2$) generated on the inner surfaces of nanopore to form stable amide bonds (Fig. 1).

These processes lead us toward the immobilization of HRP on the inner surface of a single nanopore. The realization of functionalization process was confirmed by measuring the current-voltage (I - V) of a single nanopore before and after modification (Fig. 2).

Characterization of HRP Modified Solid-State Nanopore

Here, the shape of a single Si_3N_4 nanopore channel is cylindrical. Figure 2 shows the typical current-voltage (I -

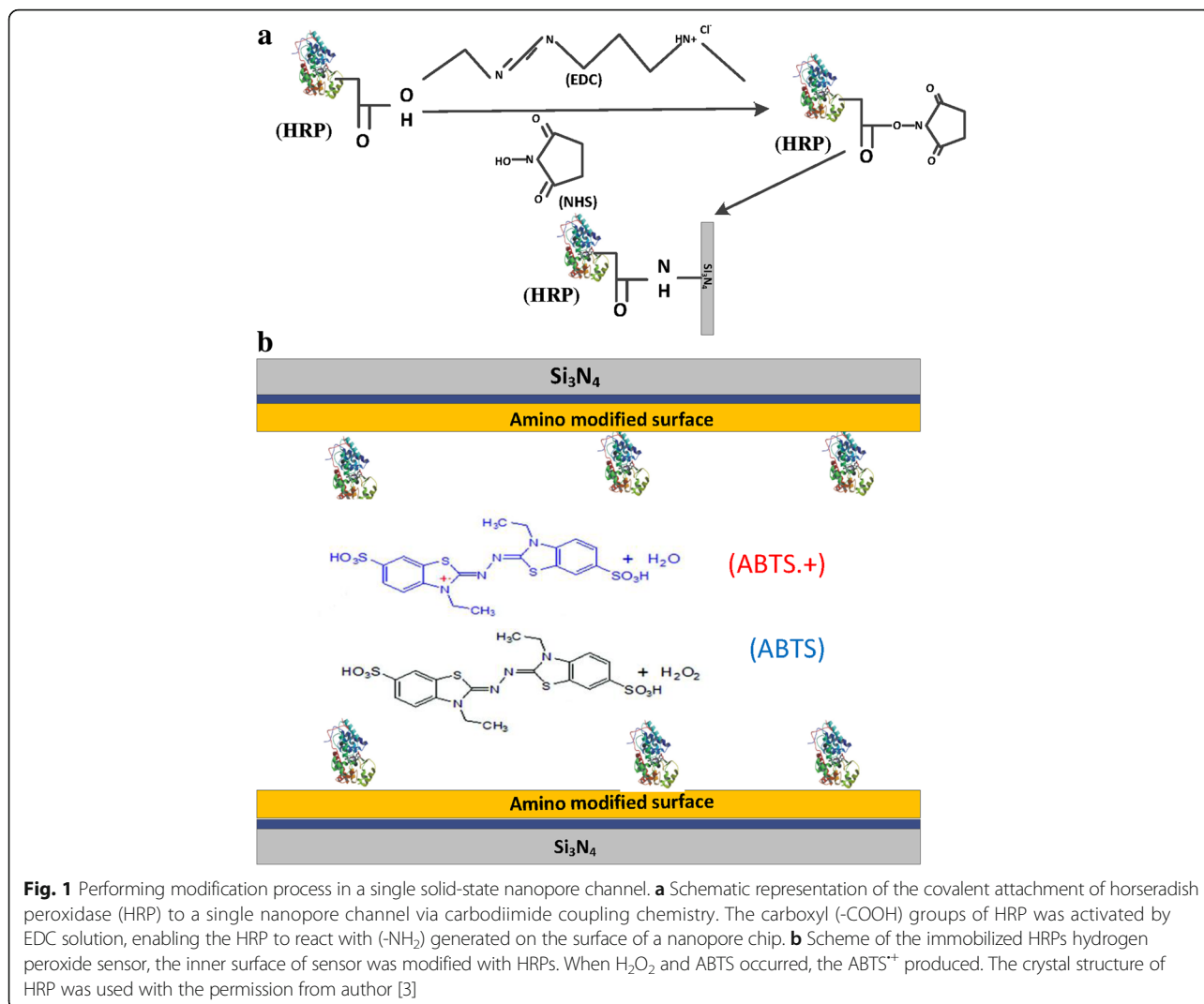


Fig. 1 Performing modification process in a single solid-state nanopore channel. **a** Schematic representation of the covalent attachment of horseradish peroxidase (HRP) to a single nanopore channel via carbodiimide coupling chemistry. The carboxyl (-COOH) groups of HRP were activated by EDC solution, enabling the HRP to react with (-NH₂) generated on the surface of a nanopore chip. **b** Scheme of the immobilized HRP hydrogen peroxide sensor, the inner surface of sensor was modified with HRP. When H₂O₂ and ABTS occurred, the ABTS⁺ produced. The crystal structure of HRP was used with the permission from author [3]

V) curves of the unmodified (original) and modified nanopore in 0.1 M KCl, buffered at pH 7.0 with 0.1 M PBS. After modifying the inner surface of nanopore with HRP enzymes, the pore size became smaller.

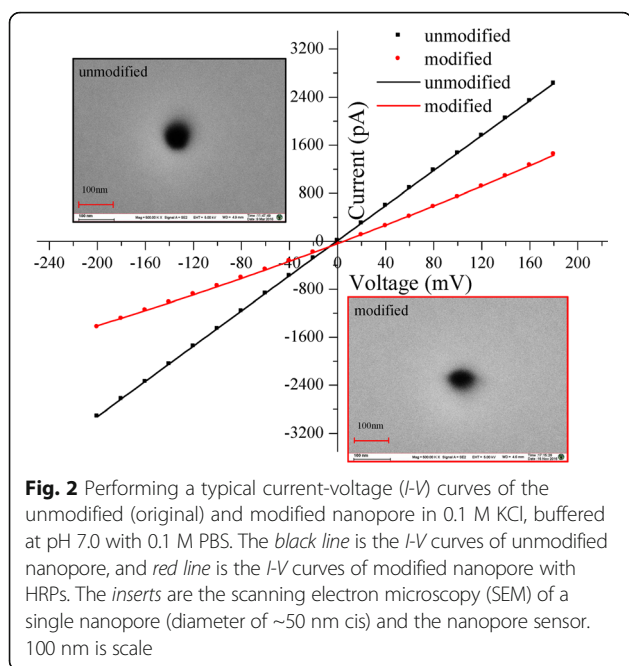
According to Wanunu et al, by taking the conductance of external of nanopore into account, diameter of solid-state nanopore can be calculated by the following equation,

$$d = \left(1 + \sqrt{1 + \frac{16\sigma l}{\pi G}} \right) G / 2\sigma \tag{1}$$

Where, *d* and *l* are the diameter and length of pore, *G* is open pore conductance of nanopore, σ is the conductivity of ion solution.

Considering geometric effects, after the modification of solid-state nanopore with HRP enzymes, effective size can be calculated. The diameter of a single nanopore can be

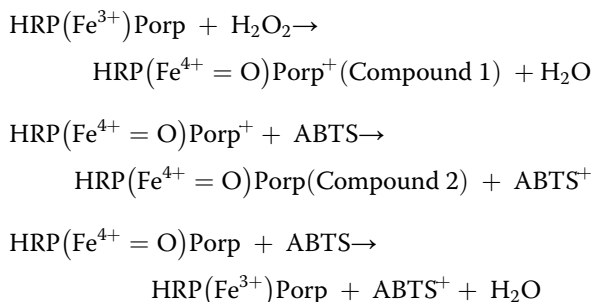
calculated based on the equation (1). Where, the value of conductance (*G_{unmodified}*) is ~15 nS can be obtained from *I-V* curves of the unmodified solid-state nanopore. The conductivity (σ) of ion solution 0.1 M KCl (25 °C), buffered at pH 7.0 with 0.1 M PBS is ~1.28 S/m. Therefore, the diameter of unmodified nanopore is ~51 nm, it is similar to the measured diameter. Using the same method, the value obtained of conductance (*G_{modified}*) is ~7.5 nS, and the diameter (~34 nm) of modified nanopore can be calculated. Reduction in diameter is possible due to the following two reasons, first is treating the inner surface of nanopore with (3-aminopropyl)triethoxysilane (3-APTES), allowing the surface of nanopore to take (-NH₂) amino groups. The second reason is that the hydrodynamic diameter (*D_h*) of HRP enzyme is ~8 nm [3], the immobilized HRP could reduce the pore's diameter. Here, the HRP modified solid-state nanopore with diameter of ~34 nm is used as the hydrogen peroxide detection channel.



The Principle of Redox Reaction

The redox reaction was conducted inside a single modified nanopore, and the following presented reaction process agrees well with the redox reaction proposed [58]. In presence of H_2O_2 (0.5 mM), HRP enzymes immobilized on the inner surface of nanopore was converted into compound 1 immediately. Then, the compound 1 accepted one electron from the reducing substrate molecule ABTS (1.5 mM) to generate compound 2. Subsequently, compound 2 was reduced back to the resting enzyme via one electron transfer from another substrate molecule ABTS.

The cationic products (ABTS^{2+}) of the redox reactions were accumulated in single nanopore. The translocation of accumulated molecules from the nanopore channel would change the conductance (G), and thus the change of current (ΔI_b) can be found.



Detection of Translocation Events

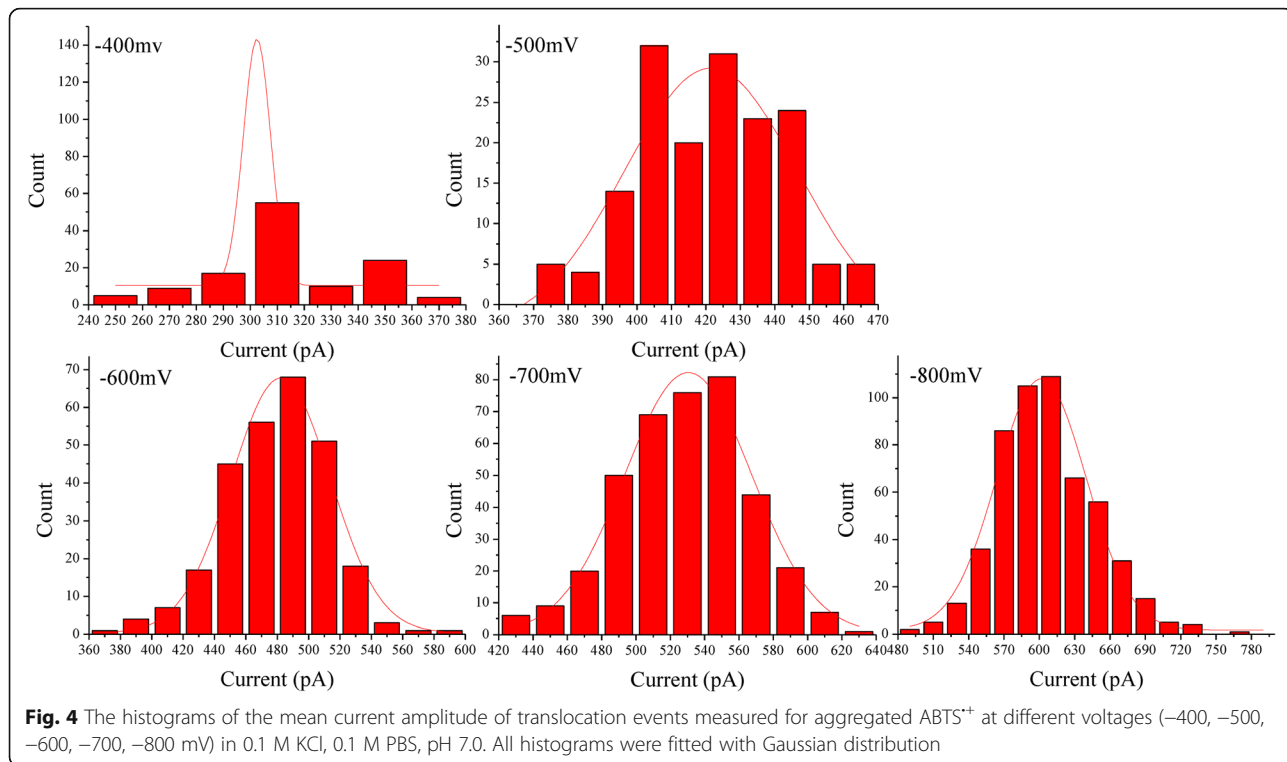
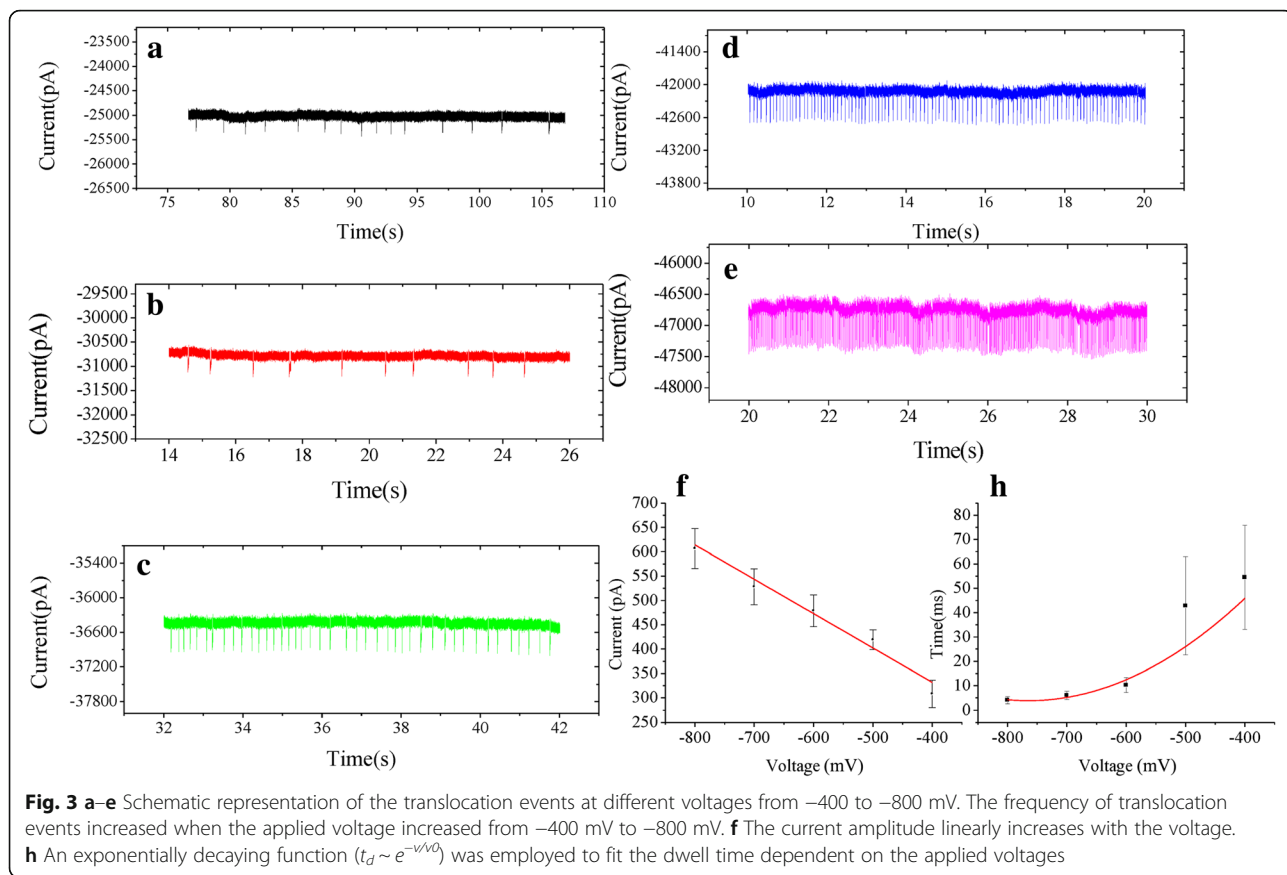
Experiments were performed using horseradish peroxidase (HRP) modified nanopores with modified pore

diameters (~34 nm) in 0.1 M KCl, buffered at pH 7.0 with 0.1 M PBS. 2, 2'-Azinobis-(3-ethylbenzthiazoline-6-sulphonate (ABTS) (1.5 mM) and hydrogen peroxide (H_2O_2) (0.5 mM) were added to the trans compartment of the nanopore. After adding ABTS and H_2O_2 , the experiments using biased voltages from -100 to -800 mV were performed, and they were sampled at 100 kHz. There were no translocation event until the voltage increased to -400 mV. Figure 3 shows representative ionic current traces of the translocation event at different voltages from -400 to -800 mV in 0.1 M KCl, 0.1 M PBS, pH 7.0. The experiments data of long duration translocation events of different voltages were added to the supplementary material (see Additional file 1: Figure S3).

The millisecond current blockade events were observed, conducted in 0.1 M KCl, 0.1 M PBS, pH 7.0. By adding the reagent H_2O_2 and ABTS into the transcompartment, HRP enzymes immobilized on the inner surface of single nanopore channel, and redox reaction occurred. Abundance of ABTS^{2+} molecules were produced, a single smaller molecule ABTS^{2+} may not be detected using our solid-state nanopore, due to the resolution of the system [3]. However, these molecules would aggregate after their production. Therefore, it is possible to detect the ABTS^{2+} molecules. Here, the negative voltages were held, and aggregated ABTS^{2+} molecules passed through the nanopores. There was an electrophoretic and electroosmotic flow when negative voltage was applied. HRP was negatively charged in 0.1 M KCl, 0.1 M PBS, pH 7.0 [3], as a result, double electrical layer would be produced, and electroosmosis would be towards negative electrode direction. Due to this reason, electrophoresis and electroosmosis were towards to the same direction. The aggregated ABTS^{2+} in the single nanopore channel would transport through the solid-state nanopore, flow toward negative electrode direction.

Statistical Analysis of Translocation Events

Since the biased voltage played a key role in translocation of aggregated ABTS^{2+} , the influence of current blockades of aggregated ABTS^{2+} passing through the HRP modified nanopore versus applied voltages was discussed. The occurrence frequency of translocation events was greatly improved with the increase in voltage (Fig. 3f). As the voltage increased, so does the amplitude of the current. However, the translocation events gradually disappeared when the biased voltage was kept below -300 mV, which suggested that aggregated ABTS^{2+} across HRP modified nanopores needed a -300 mV threshold voltage. Figure 4 shows histograms of the mean current amplitude of translocation events measured for aggregated ABTS^{2+} at different voltages. Based on the fitting curves, the peak values of the current blockade (ΔI_b) are 308.4 ± 27.795 pA, 419.1 ± 20.354 pA,



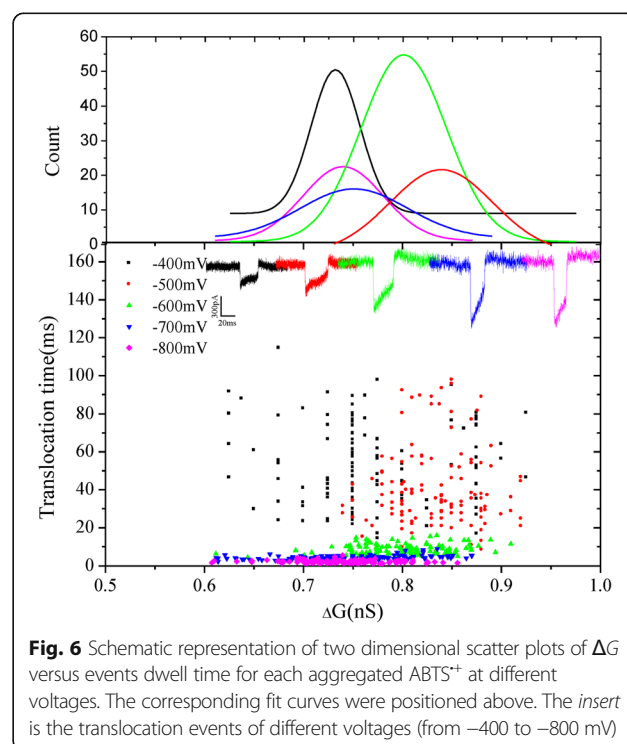
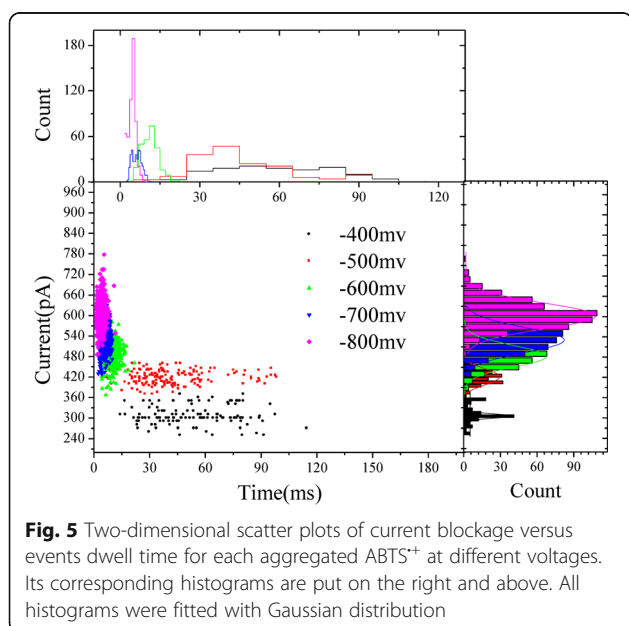
478.8 ± 32.857 pA, 528.1 ± 36.98 pA, 606.9 ± 40.916 pA at -400, -500, -600, -700, and -800 mV, respectively, it is likely that the reduction of current is induced by aggregated ABTS^{•+} molecule passing through the nanopore at different voltages. The values of current amplitude were fitted with a first-order polynomial function, which produces a slope of -0.706 and intercept of 49.262. However, based on the fitting curves, the values of dwell time are 54.5 ± 21.374 ms, 42.8 ± 20.181 ms, 10.3 ± 3.05 ms, 6.0 ± 1.744 ms, 4.0 ± 1.441 ms, at -400, -500, -600, -700, and -800 mV. Figure 3h shows an exponentially decaying function ($t_d \sim e^{-v/v_0}$) was employed to fit the dwell time dependent on the applied voltages. The histograms of the dwell time of translocation events were added to the supplementary material (see Additional file 1: Figure S4).

The current blockade versus events dwell time for each aggregated ABTS^{•+} at different voltages were fitted in two dimensional scatter plots (Fig. 5). All of the aggregated ABTS^{•+} show a cluster of events from -400 to -800 mV, the main event clusters are due to aggregated ABTS^{•+} passing through the HRP modified solid-state nanopore.

In addition, the single translocation event at every voltage was analysed, and the current blockade was induced by the same size and charged substance. So, it is deemed that every translocation event was induced by the single aggregated ABTS^{•+}. To analyse the translocation time of aggregated ABTS^{•+} in our experiments. The current blockade duration t_d is regarded as the dwell time of a single aggregated ABTS^{•+} from the location where it produced to the exit of nanopore. Here, another condition was considered, there may be some HRP

enzymes immobilized on the entrance of nanopore, and it might catalyse the redox reaction. Therefore, other experiments were conducted to verify that the redox reaction occurred at the inner surface of a single nanopore rather than at the entrance. For the verification, unmodified by HRPs were applied and analysed. These nanopores were activated with 3-APTES. And the same concentration HRPs (10 ng/ml), ABTS (1.5 mM) and H₂O₂ (0.5 mM) were added to the trans compartment of nanopore, the negative biased voltage was applied in 0.1 M KCl, 0.1 M PBS, pH 7.0, due to the electrophoresis force, HRPs were unable to pass through the nanopore. Owing to the redox reaction, the aggregated ABTS^{•+} produced, but there were no translocation events found. It is possible that the aggregated ABTS^{•+} cause electrostatic effect with HRPs and prevent the aggregated ABTS^{•+} passing through the nanopore.

Figure 6 shows the two dimensional scatter plots of the change of conductance (ΔG) versus events dwell time for each aggregated ABTS^{•+} at different voltages. It can be found that change of conductance (ΔG) mainly concentrated in 0.8 nS. The shape of translocation events are almost the same. The mean value of ΔG is ~0.8 nS at different voltages. It can be speculated that the volume exclusion of every aggregated ABTS^{•+} molecule is almost same. It is possible that electrostatic and steric effects of aggregated ABTS^{•+} molecules may change the ionic current. After the analysis, two typical shapes of current traces with the positive charged



aggregated ABTS^{•+} translocation were observed (Fig. 7). The translocation events at -700 mV as a representative. The percentage of two type events were analysed, and it can be observed that the percentage of type 1 events increased with the increase in voltage, on the other hand, the percentage of type 2 events was decreased. It was considered that higher voltage make the translocation faster than the lower voltage.

The current blockade signals revealed the size, conformation, and interaction of aggregated ABTS^{•+} passing through the single nanopore channel. For the change in current shape, the process of the changes were speculated. For the event 1, current signals have a typical fluctuation part with a deep intensity and a short dwell time. It is possible that the aggregated ABTS^{•+} passed through the nanopore from the place where it is produced. When the aggregated ABTS^{•+} passed through the nanopore, the ionic current of nanopore restored to the original level (Baseline) (I_0). For the event 2, the current signals have a fluctuation part with a deep intensity and then have a horizontal stage. This shape of signals can be attributed to the electrostatic interaction of aggregated ABTS^{•+} with the HRP at the exit of nanopore, and current was slowly recovered to the baseline. For better understanding of current change, we need to start with the open pore conductance change (G_{pore}) at salt concentration (0.1 M KCl). As discussed in the previous studies, an equation of the open pore conductance of a negatively charged nanopore with a diameter of d and a length of l at low salt concentration can be described as

$$G_{pore} = \frac{\pi d^2_{pore}}{4l_{pore}} \left[(\mu_{K^+} + \mu_{Cl^-}) n_{KCl} \cdot e + \mu_K \frac{4\sigma_p}{d_{pore}} \right] \quad (2)$$

where μ_K and μ_{Cl^-} are the electrophoretic motilities of K^+ and Cl^- , n_{KCl} is the number density of K^+ and Cl^- , the

elementary charge is e , σ_p is the surface charge density of the nanopore surfaces. In this experiment, the solid-state nanopore was chemically modified, and diameter of nanopore was changed. The surface charge density of the nanopore surface (σ_p) cannot be obtained exactly. Therefore, the open pore conductance (G_{pore}) was calculated based on equation (1). On account of equation (1), the open pore conductance (G_{pore}) is ~ 7.5 nS. It is speculated that the change of conductance can be attributed to two reasons [15]. The first reason is that, the volume exclusion of ions in nanopore were occupied by the aggregated ABTS^{•+} molecules. As a result, the conductance of solid-state nanopore was decreased (ΔG^-). The second reason is that, some ions were brought from the nanopore by the aggregated ABTS^{•+} molecules which increased the conductance of solid-state nanopore. In these experiments, the ABTS^{•+} produced inside nanopore, and no ions were brought. Therefore, the change in the conductance of solid-state nanopore (ΔG) was only induced by the volume exclusion. So, the total change of the conductance can be described as

$$\Delta G = \Delta G^- \quad (3)$$

The decrease in the conductance of solid-state nanopore is induced by the volume exclusion and it can be calculated by the following equation

$$\Delta G^- = \sigma \frac{\gamma \Lambda}{(l + 0.8d)^2} \quad (4)$$

where γ is particle shape factor which is the surface areas ratio of the same volume spherical and the particle. In this work, the aggregated ABTS^{•+} molecule was simplified to a global object, therefore the value of γ is 1 and Λ is the volume exclusion. The conductivity of bulk solution σ is 1.28 S/m, 0.1 M KCl (25 °C).

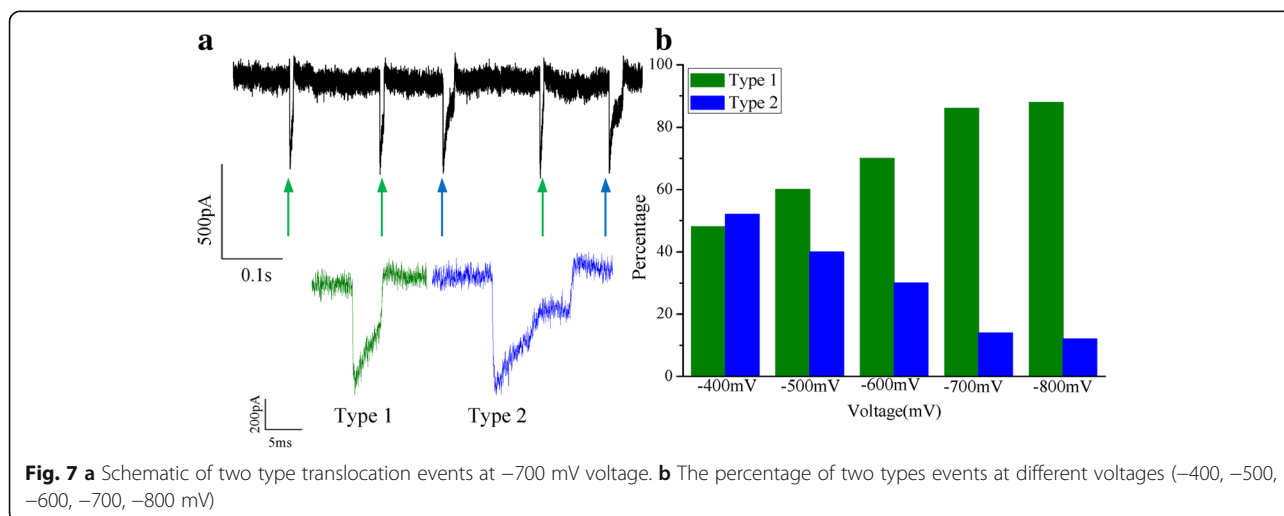


Fig. 7 a Schematic of two type translocation events at -700 mV voltage. b The percentage of two types events at different voltages (-400, -500, -600, -700, -800 mV)

For the volume exclusion (Λ), we can deduce from the translocation events of some other molecules. For connecting the conductance change (ΔG) to the physical property of molecules, Ohm's Law can be applied to the volume change of electrolyte solution based on the solid-state nanopore [59]. When a translocation event of a molecule in a cylindrical solid-state nanopore, the current decreased instantaneously. When the resistance of solid-state nanopore is the whole circuit resistance, the conductance change (ΔG) can be described by the following equation

$$\Delta G(t) = -G_{pore} \frac{\Lambda(t)}{H_{eff} A_p} [1 + f(d_m/D_p, l_m/H_{eff})] \quad (5)$$

In this equation, A_p , $H_{eff} = V_p$ is the volume of solid-state nanopore, $f(d_m/D_p, l_m/H_{eff})$ is correction factor (it ignored the surface charge effect), in our experiments, we simplified the aggregated ABTS^{•+} molecule to a global object; therefore, the correction factor is 1. The d_m/D_p is the ratio of molecule diameter and nanopore diameter, The l_m/H_{eff} is ratio of molecule effective length and nanopore effective length. The expression (5) can be simplified as

$$\Delta G/G_{pore} \approx \Lambda/V_p \quad (6)$$

The mean value of conductance (G_{pore}) has been analysed of translocation events. From the equation (5), the mean value of volume exclusion (Λ) at different voltages (-400, -500, -600, -700, -800 mV) can be obtained. Meanwhile, the size of the used nanopore is known, the volume of nanopore (V_p) is $\sim 90746 \text{ nm}^3$. On account of equation (4), the value of conductance change (ΔG) can be calculated as $\sim 0.6 \text{ nS}$. The mean value of conductance change that obtained from the translocation events experiments at different voltages (-400, -500, -600, -700, -800 mV) is $\sim 0.784 \text{ nS}$. It can be found that the calculated value is near to the experimental value.

In some previous investigation, hydrogen peroxide molecules have been achieved to be detected with different technologies. But, to detect hydrogen peroxide by nanochannel is rare. Tan et al. [3] differentiated disparate event signals when HRPs threaded into nanopore, there were ABTS and H_2O_2 in KCl solution. The different type signals with HRPs translocation were regarded as ABTS^{•+} passing through nanopore. Six typical events of the translocation of the product of enzyme catalysis substrates were analyzed. They speculated the probable process of every type. However, no enough evidences to testify. Mubarak Ali et al. have accomplished to detect the redox reaction products inner single conical nanochannels [58]. They found that the cationic radical ABTS^{•+} reduced the ion current in the HRP-nanochannel in a voltage-dependent fashion, consistent with voltage-

dependent concentrations of ions in conical nanochannels. The magnitude of the current blockage was correlated with the H_2O_2 concentration in the solution.

Conclusions

In conclusion, we fabricated a Si_3N_4 nanopore employing a FIB successfully, a single nanopore system whose surface was modified with covalently linked HRP enzymes. The effect of the immobilized HRPs enzymes in a single solid-state nanopore as a hydrogen peroxide (H_2O_2) sensor was affirmed by investigating products (ABTS^{•+}) of the redox reactions occurring in presence of the substrates H_2O_2 and ABTS. The aggregated cationic radical ABTS^{•+} produced inside the solid-state nanopore and reduced the ionic current in the HRPs modified solid-state nanopore, are consistent with voltage-dependence. The current blockade trends showed linear dependence for applied biased voltages. The relationship between the dwell time versus applied biased voltage was the exponentially decaying ($t_d \sim e^{-v/v_0}$). Meanwhile, the aggregated ABTS^{•+} passed through the HRPs modified nanopores needed a -300 mV threshold voltage. The change of conductance (ΔG) has been calculated analytically and compared to the measured experimental values. The translocation events were produced by the certain size aggregated cationic radical ABTS^{•+}. We expect that using solid-state nanopores will allow lowering the detection limit and improve the system sensitivity. For our solid-state nanopore system, the structure is simple; it is not susceptible to fouling and can be used multiple times.

Additional file

Additional file 1: The instruments of our experiments used. **Figure S1.** The system include an Axopatch 700B (Molecular Devices, Inc., Sunnyvale, CA, USA). A double Faraday cage enclosure. The apparatus of our experiments used. **Figure S2.** The pictures of a custom-built Teflon cell with two Viton o-rings to separate the two side of chip. 1 Joint; 2 Teflon cell; 3 M5 plastic screw; 4 Viton o-rings. The experiments data of long duration translocation events of different voltages. **Figure S3.** The experiments data of long duration translocation events of different voltages from -400 to -800 mV in 0.1M KCl, 0.1 M PBS, pH 7.0. The histograms of the dwell time of translocation events. **Figure S4.** The histograms of the dwell time of translocation events. Based on the fitting curves, the values of dwell time are $54.5 \pm 21.374 \text{ ms}$, $42.8 \pm 20.181 \text{ ms}$, $10.3 \pm 3.051 \text{ ms}$, $6.0 \pm 1.744 \text{ ms}$, $4.0 \pm 1.441 \text{ ms}$, at -400, -500, -600, -700, and -800 mV. The SEM images of nanopore silicon nitride thin film deposited on Si wafer. **Figure S5.** (a) The picture of experiments used Si_3N_4 nanopore. (b) The SEM image of nanopore silicon nitride thin film deposited on Si substrate. (c) (d) The SEM images of nanopore silicon nitride thin film and broken silicon nitride thin film. (e) The process of nanopore fabrication. (DOCX 2737 kb)

Abbreviations

3-APTES: (3-Aminopropyl)triethoxysilane; ABTS: 3-ethylbenzothiazoline-6-sulfonic acid; EDC: N-(3-dimethylaminopropyl)-N'-ethylcarbodiimide; FIB: Focused ion beam; HRP: Horseradish peroxidase; KCl: Potassium chloride; NHS: N-hydroxysuccinimide; SEM: Scanning electron microscopy; SNR: Signal to noise ratio

Acknowledgements

The authors gratefully acknowledge financial support from the National Key Research and Plan of China (2016YFA0501602) and the National Natural Science Foundation of China (61372031).

Authors' Contributions

LZ and QL designed the experiments. LZ did the chemical modification and nanopore experiments and drafted the manuscript. DG participated in the solid-state nanopore fabrication. LZ and DG participated in the analysis. All authors read and approved the final manuscript.

Competing Interests

The authors declare that they have no competing interests.

About the Authors

Libo Zhu is Ph.D candidate in Biomedical engineering, State Key Laboratory of Bioelectronics, school of biological science and medical engineering, Southeast University, Nanjing, PR China. Mainly interested in a new generation of gene sequencing, nanopore sensors, single molecule detection research.

Dejian Gu is currently pursuing his Master's degree in Southeast University, Nanjing, China. The major of study is the third sequencing of nanopore. Qianjun Liu is Professor in Biomedical engineering in Southeast University, Nanjing, China. Mainly interested in a new generation of gene sequencing, gene chip, biological and chemical sensors, single molecule detection research.

Publisher's Note

Springer Nature remains neutral with regard to jurisdictional claims in published maps and institutional affiliations.

Received: 5 March 2017 Accepted: 8 June 2017

Published online: 20 June 2017

References

- Coulter W (1953) Means for counting particles suspended in a fluid. US Patent, 2656508. United States Patent Office Patentiert am 20:1953
- Cornell BA, Braach-Maksytis V, King L, Osman P (1997) A biosensor that uses ion-channel switches. *Nature* 387:580
- Tan S, Gu D, Liu H, Liu Q (2016) Detection of a single enzyme molecule based on a solid-state nanopore sensor. *Nanotechnology* 27:155502
- Jubery TZ, Prabhu AS, Kim MJ, Dutta P (2012) Modeling and simulation of nanoparticle separation through a solid-state nanopore. *Electrophoresis* 33:325–33
- Kong J, Wu H, Liu L, Xie X, Wu L, Ye X, Liu Q (2013) Silicon nitride nanopores for nanoparticle sensing. *J Nanosci Nanotechnol* 13:4010–6
- Liu Q, Yao H, Wang L, Hou C, Zhao W (2014) Translocation of gold nanorod through a solid-state nanopore. *Sci Adv Mater* 6:2075–8
- Liu L, Wu H, Kong J, Liu Q (2013) Solid-state nanopore for rod-like virus detection. *Sci Adv Mater* 5:2039–47
- McMullen A, De Haan HW, Tang JX, Stein D (2014) Stiff filamentous virus translocations through solid-state nanopores. *Nat Commun* 5:4171.
- Miao W, Liu L, Lu A, Wu H, Sharma P, Dogic Z, Ling X (2014) Effects of ionic strength on nonlinear electrophoretic mobility of fd virus in solid-state nanopore (vol 1), p 20009
- Cressiot B, Oukhaled A, Patriarche G, Pastoriza-Gallego M, Betton J-M, Auvray LC, Muthukumar M, Bacri L, Pelta J (2012) Protein transport through a narrow solid-state nanopore at high voltage: experiments and theory. *ACS Nano* 6:6236–43
- Firnkes M, Pedone D, Knezevic J, Döblinger M, Rant U (2010) Electrically facilitated translocations of proteins through silicon nitride nanopores: conjoint and competitive action of diffusion, electrophoresis, and electroosmosis. *Nano Lett* 10:2162–7
- Hsu WL, Daiguji H (2016) Manipulation of Protein Translocation through Nanopores by Flow Field Control and Application to Nanopore Sensors. *Anal Chem* 88:9251–8
- Wu L, Liu H, Zhao W, Wang L, Hou C, Liu Q, Lu Z (2014) Electrically facilitated translocation of protein through solid nanopore. *Nanoscale Res Lett* 9:1–10
- Tan S, Wang L, Yu J, Hou C, Jiang R, Li Y, Liu Q (2015) DNA-functionalized silicon nitride nanopores for sequence-specific recognition of DNA biosensor. *Nanoscale Res Lett* 10:205
- Smeets RM, Keyser UF, Krapf D, Wu M-Y, Dekker NH, Dekker C (2006) Salt dependence of ion transport and DNA translocation through solid-state nanopores. *Nano Lett* 6:89–95
- Plesa C, van Loo N, Ketterer P, Dietz H, Dekker C (2014) Velocity of DNA during translocation through a solid-state nanopore. *Nano Lett* 15:732–7
- Liu Q, Wu H, Wu L, Xie X, Kong J, Ye X, Liu L (2012) Voltage-driven translocation of DNA through a high throughput conical solid-state nanopore. *PLoS One* 7:e46014
- Stefureac R, Waldner L, Howard P, Lee JS (2008) Nanopore Analysis of a Small 86-Residue Protein. *Small* 4:59–63
- Oukhaled G, Mathe J, Bianca A-L, Bacri L, Betton J-M, Lairez D, Pelta J, Auvray L (2007) Unfolding of proteins and long transient conformations detected by single nanopore recording. *Phys Rev Lett* 98:158101
- Cressiot B, Braselmann E, Oukhaled A, Elcock AH, Pelta J, Clark PL (2015) Dynamics and energy contributions for transport of unfolded pertactin through a protein nanopore. *ACS Nano* 9:9050–61
- Pastoriza-Gallego M, Rabah L, Gibrat G, Thiebot B, van der Goot FG, Auvray L, Betton J-M, Pelta J (2011) Dynamics of unfolded protein transport through an aerolysin pore. *J Am Chem Soc* 133:2923–31
- Stefureac R, Y-t L, Kraatz H-B, Howard P, Lee JS (2006) Transport of α -helical peptides through α -hemolysin and aerolysin pores. *Biochemistry* 45:9172–9
- Asandei A, Chinappi M, Kang H-K, Seo CH, Mereuta L, Park Y, Luchian T (2015) Acidity-mediated, electrostatic tuning of asymmetrically charged peptides interactions with protein nanopores. *ACS Appl Mater Interfaces* 7:16706–14
- Hernandez-Ainsa S, Misiunas K, Thacker W, Hemmig EA, Keyser UF (2014) Voltage-dependent properties of DNA origami nanopores. *Nano Lett* 14:1270–4
- Hoogerheide DP, Lu B, Golovchenko JA (2014) Pressure–voltage trap for DNA near a solid-state nanopore. *ACS Nano* 8:7384–91
- Li J, Fologea D, Rollings R, Ledden B (2014) Characterization of protein unfolding with solid-state nanopores. *Protein Pept Lett* 21:256–65
- Kowalczyk SW, Hall AR, Dekker C (2009) Detection of local protein structures along DNA using solid-state nanopores. *Nano Lett* 10:324–8
- Freedman KJ, Haq SR, Edel JB, Jemth P, Kim MJ (2013) Single molecule unfolding and stretching of protein domains inside a solid-state nanopore by electric field. *Sci Rep* 3:1638
- Li W, Bell NA, Hernández-Ainsa S, Thacker W, Thackray AM, Bujdosó R, Keyser UF (2013) Single protein molecule detection by glass nanopores. *ACS Nano* 7:4129–34
- Ding S, Gao C, Gu L-Q (2009) Capturing single molecules of immunoglobulin and ricin with an aptamer-encoded glass nanopore. *Anal Chem* 81:6649–55
- Freedman KJ, Bastian AR, Chaiken I, Kim MJ (2013) Solid-state nanopore detection of protein complexes: applications in healthcare and protein kinetics. *Small* 9:750–9
- Oukhaled A, Cressiot B, Bacri L, Pastoriza-Gallego M, Betton J-M, Bourhis E, Jede R, Gierak J, Auvray LC, Pelta J (2011) Dynamics of completely unfolded and native proteins through solid-state nanopores as a function of electric driving force. *ACS Nano* 5:3628–38
- Niedzwiecki DJ, Grazul J, Movileanu L (2010) Single-molecule observation of protein adsorption onto an inorganic surface. *J Am Chem Soc* 132:10816–22
- Ali M, Schiedt B, Healy K, Neumann R, Ensinger W (2008) Modifying the surface charge of single track-etched conical nanopores in polyimide. *Nanotechnology* 19:085713
- Gyurcsányi RE (2008) Chemically-modified nanopores for sensing. *Trends Anal Chem* 27:627–39
- Nilsson J, Lee JRI, Ratto TV, Létant SE (2006) Localized Functionalization of Single Nanopores. *Adv Mater* 18:427–31
- Perez-Mitta G, Burr L, Tuninetti JS, Trautmann C, Tomil-Molares ME, Azzaroni O (2016) Noncovalent functionalization of solid-state nanopores via self-assembly of amphipols. *Nanoscale* 8:1470–8
- Prabhu AS, Jubery TZ, Freedman KJ, Mulero R, Dutta P, Kim MJ (2010) Chemically modified solid state nanopores for high throughput nanoparticle separation. *J Phys Condens Matter* 22:454107
- Shan Y, Tiwari P, Krishnakumar P, Vlassiokou I, Li W, Wang X, Darici Y, Lindsay S, Wang H, Smirnov S (2013) Surface modification of graphene nanopores for protein translocation. *Nanotechnology* 24:495102
- Tang Z, Lu B, Zhao Q, Wang J, Luo K, Yu D (2014) Surface modification of solid-state nanopores for sticky-free translocation of single-stranded DNA. *Small* 10:4332–9
- Wei R, Gatterdam V, Wieneke R, Tampé R, Rant U (2012) Stochastic sensing of proteins with receptor-modified solid-state nanopores. *Nat Nanotechnol* 7:257–63

42. Chang Q, Zhu L, Jiang G, Tang H (2009) Sensitive fluorescent probes for determination of hydrogen peroxide and glucose based on enzyme-immobilized magnetite/silica nanoparticles. *Anal Bioanal Chem* 395:2377–85
43. Dickinson BC, Huynh C, Chang CJ (2010) A palette of fluorescent probes with varying emission colors for imaging hydrogen peroxide signaling in living cells. *J Am Chem Soc* 132:5906–15
44. Jin H, Heller DA, Kalbacova M, Kim J-H, Zhang J, Boghossian AA, Maheshri N, Strano MS (2010) Detection of single-molecule H₂O₂ signalling from epidermal growth factor receptor using fluorescent single-walled carbon nanotubes. *Nat Nanotechnol* 5:302–9
45. Srikun D, Albers AE, Nam CI, Iavarone AT, Chang CJ (2010) Organelle-targetable fluorescent probes for imaging hydrogen peroxide in living cells via SNAP-Tag protein labeling. *J Am Chem Soc* 132:4455–65
46. Chen W, Li B, Xu C, Wang L (2009) Chemiluminescence flow biosensor for hydrogen peroxide using DNAzyme immobilized on eggshell membrane as a thermally stable biocatalyst. *Biosens Bioelectron* 24:2534–40
47. Qin W, Zhang Z, Li B, Liu S (1998) Chemiluminescence flow-sensing system for hydrogen peroxide with immobilized reagents. *Anal Chim Acta* 372:357–63
48. Diaz AN, Peinado MR, Minguez MT (1998) Sol-gel horseradish peroxidase biosensor for hydrogen peroxide detection by chemiluminescence. *Anal Chim Acta* 363:221–7
49. Tahirović A, Čopra A, Omanović-Miklićanin E, Kalcher K (2007) A chemiluminescence sensor for the determination of hydrogen peroxide. *Talanta* 72:1378–85
50. Bustos Bustos E, Chapman TW, Rodríguez-Valadez F, Godínez LA (2006) Amperometric Detection of H₂O₂ Using Gold Electrodes Modified with Starburst PAMAM Dendrimers and Prussian Blue. *Electroanalysis* 18:2092–8
51. Kausaitė-Minkstimiene A, Mazeiko V, Ramanavičienė A, Ramanavičius A (2010) Enzymatically synthesized polyaniline layer for extension of linear detection region of amperometric glucose biosensor. *Biosens Bioelectron* 26:790–7
52. Nakabayashi Y, Yoshikawa H (2000) Amperometric biosensors for sensing of hydrogen peroxide based on electron transfer between horseradish peroxidase and ferrocene as a mediator. *Anal Sci* 16:609–13
53. Quintino MS, Winnischofer H, Araki K, Toma HE, Angnes L (2005) Cobalt oxide/tetraruthenated cobalt-porphyrin composite for hydrogen peroxide amperometric sensors. *Analyst* 130:221–6
54. Lee D-Y, Park S-H, Qian D-J, Kwon Y-S (2009) Electrochemical detection of hydrogen peroxide via hemoglobin-DNA/pyterpy-modified gold electrode. *Curr Appl Phys* 9:e232–e4
55. Peng Y, Jiang D, Su L, Zhang L, Yan M, Du J, Lu Y, Liu Y-N, Zhou F (2009) Mixed monolayers of ferrocenylalkanethiol and encapsulated horseradish peroxidase for sensitive and durable electrochemical detection of hydrogen peroxide. *Anal Chem* 81:9985–92
56. Razmi H, Mohammad-Rezaei R, Heidari H (2009) Self-Assembled Prussian Blue Nanoparticles Based Electrochemical Sensor for High Sensitive Determination of H₂O₂ in Acidic Media. *Electroanalysis* 21:2355–62
57. Shi C-G, Xu J-J, Chen H-Y (2007) Electrogenerated chemiluminescence and electrochemical bi-functional sensors for H₂O₂ based on CdS nanocrystals/hemoglobin multilayers. *J Electroanal Chem* 610:186–92
58. Ali M, Tahir MN, Siwy Z, Neumann R, Tremel W, Ensinger W (2011) Hydrogen peroxide sensing with horseradish peroxidase-modified polymer single conical nanochannels. *Anal Chem* 83:1673–80
59. Bezrukov S (2000) Ion channels as molecular Coulter counters to probe metabolite transport. *J Membr Biol* 174:1–13

Submit your manuscript to a SpringerOpen[®] journal and benefit from:

- Convenient online submission
- Rigorous peer review
- Open access: articles freely available online
- High visibility within the field
- Retaining the copyright to your article

Submit your next manuscript at ► springeropen.com
